



*Supplement of*

## **Tracing the contribution of dust origins on deposition and phytoplankton carbon uptake in global oceans**

**Yaxin Liu et al.**

*Correspondence to:* Jialei Zhu ([zhujialei@tju.edu.cn](mailto:zhujialei@tju.edu.cn))

The copyright of individual parts of the supplement might differ from the article licence.

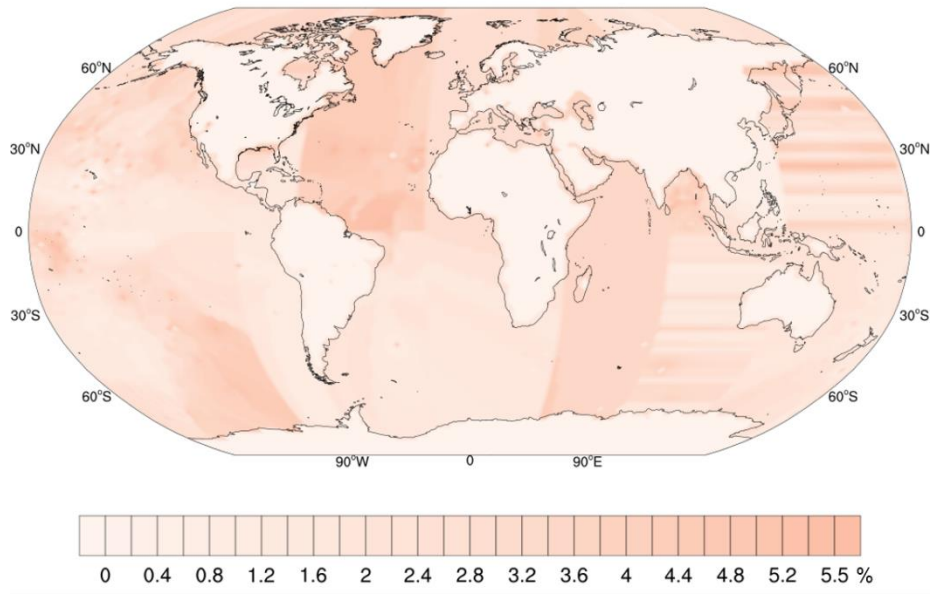


Fig. S1 The interpolated iron solubility data.

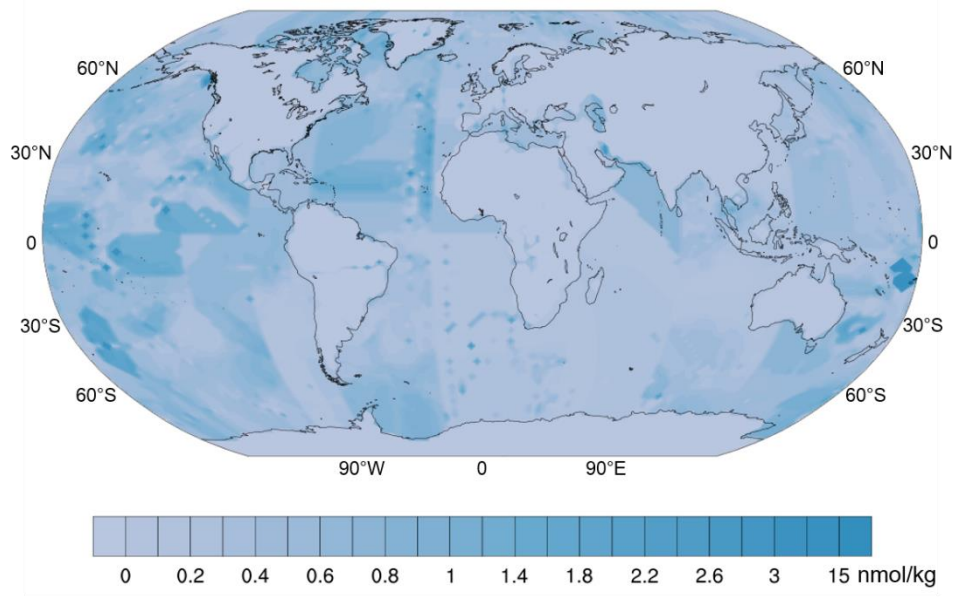


Fig. S2 The interpolated dissolved iron data.

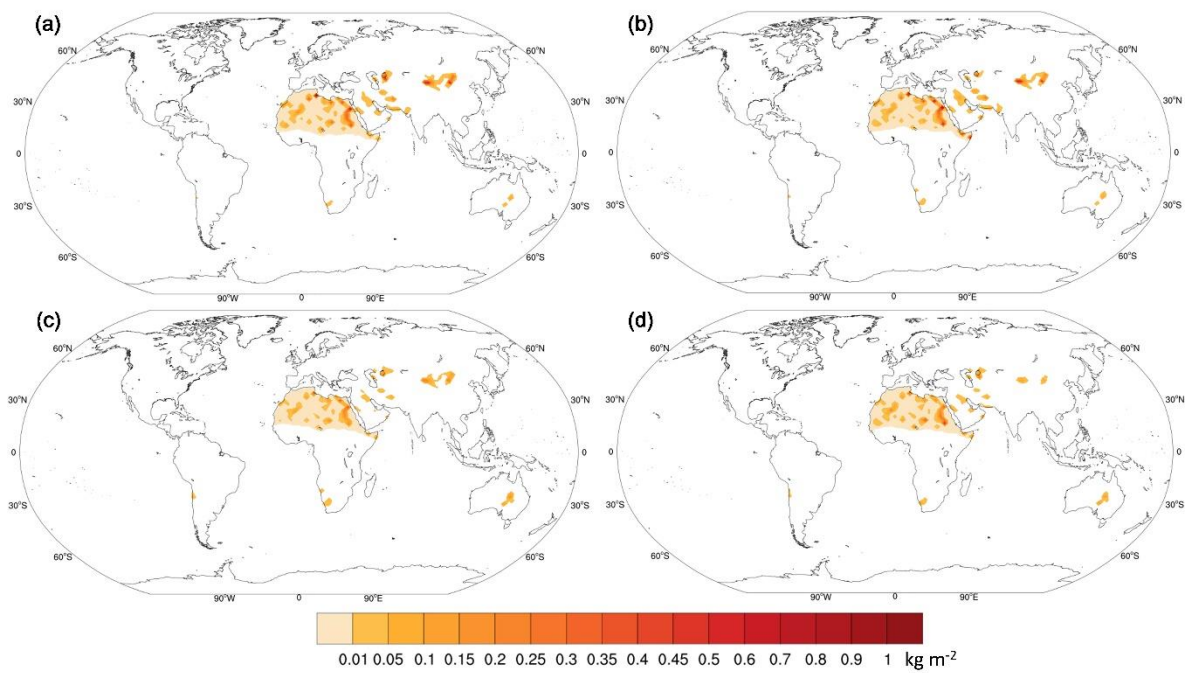


Fig.S3 Seasonal distribution of dust emission from global main dust source regions  
(a) spring; (b) summer; (c) autumn; (d) winter

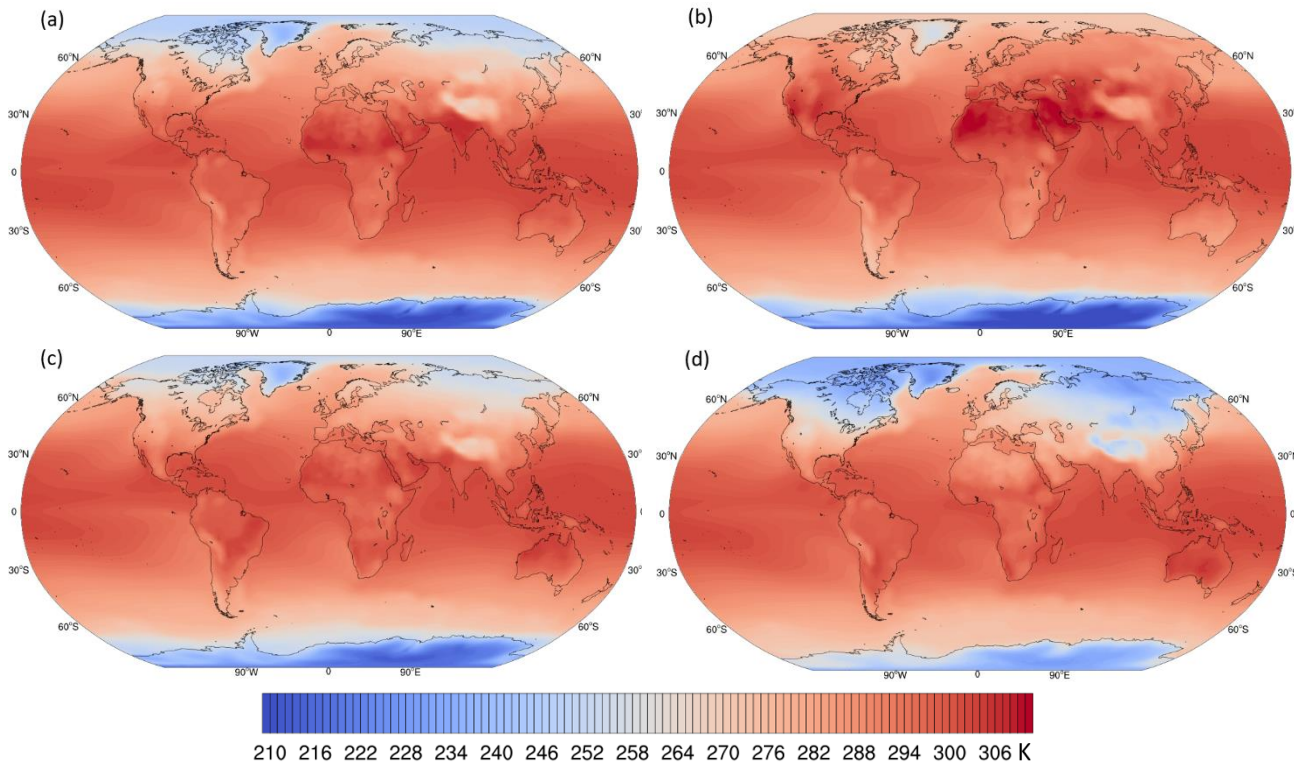


Fig.S4 Seasonal characteristics of global surface temperature  
 (a) spring; (b) summer; (c) autumn; (d) winter

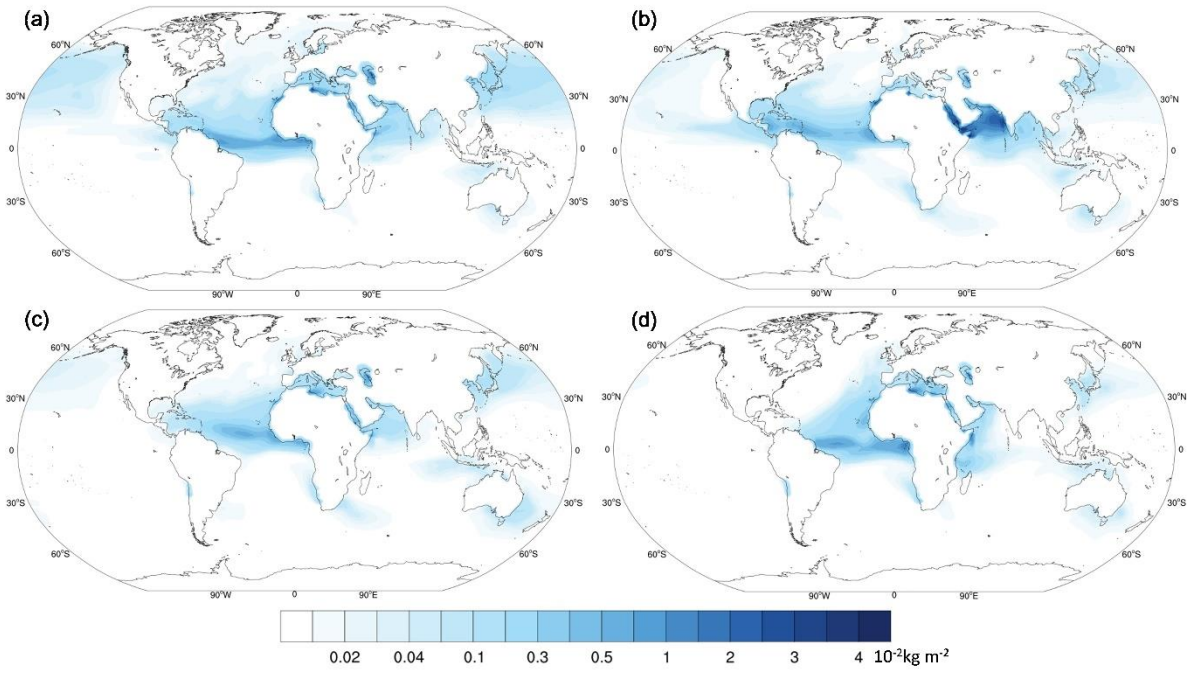


Fig.S5 Seasonal distribution of global marine dust deposition  
(a) spring; (b) summer; (c) autumn; (d) winter

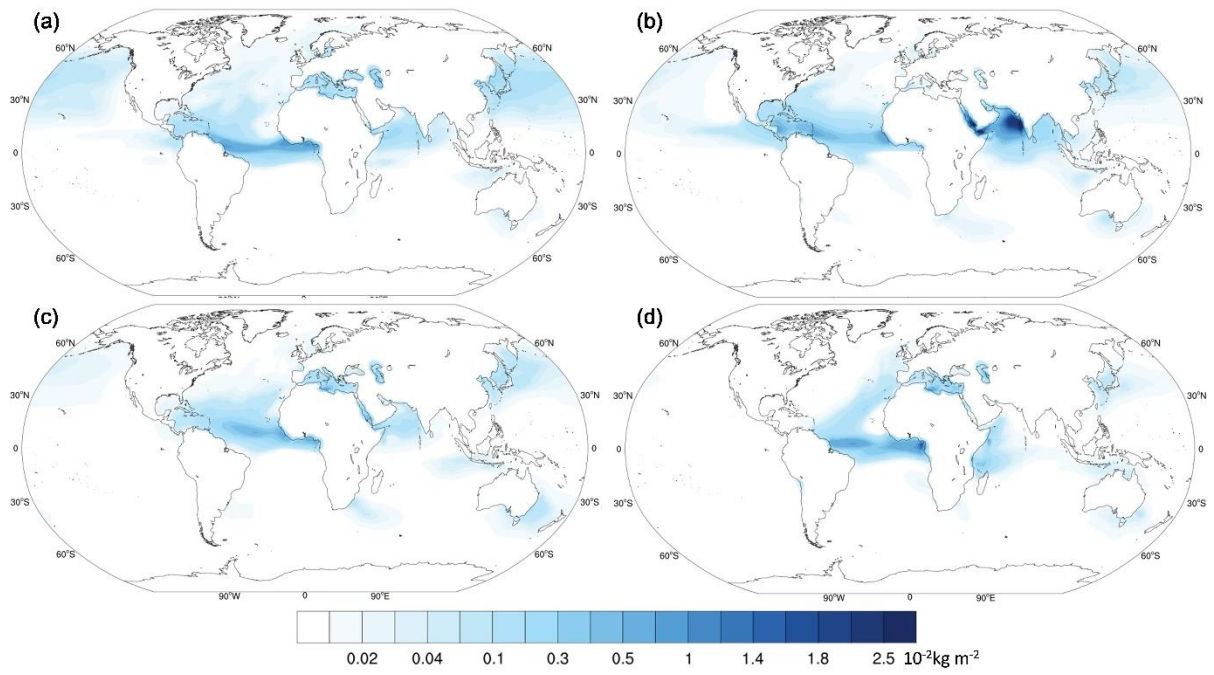


Fig.S6 Seasonal distribution of global marine dust wet deposition  
(a) spring; (b) summer; (c) autumn; (d) winter



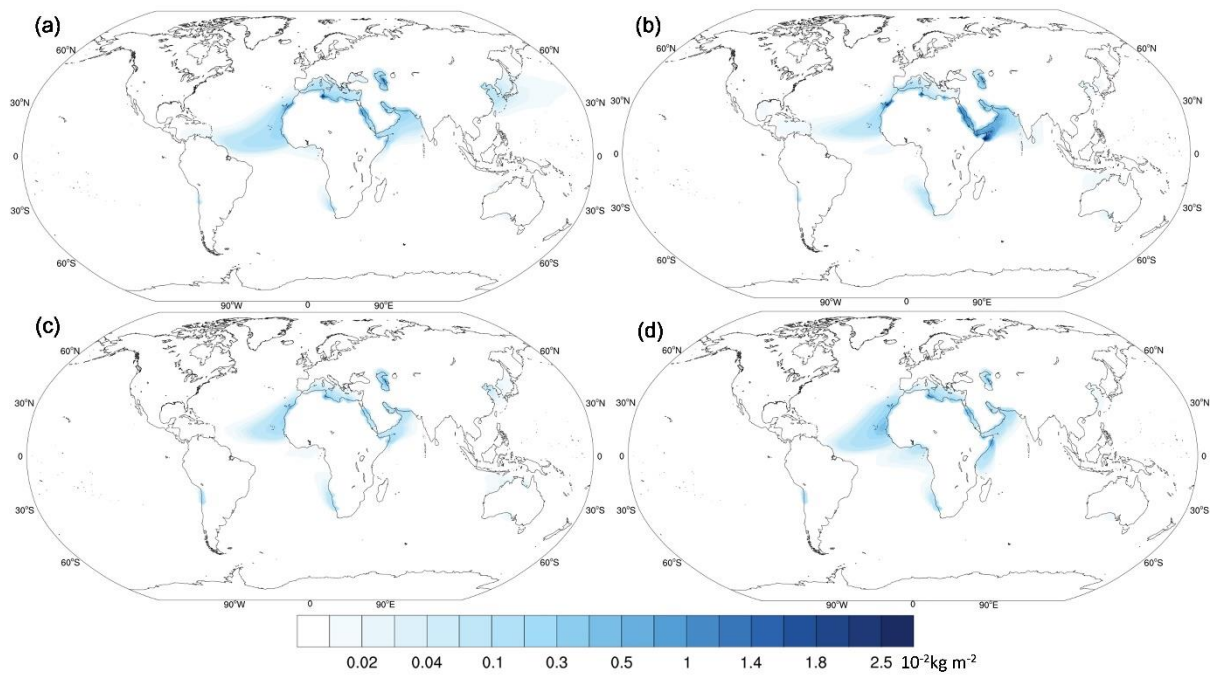


Fig.S7 Seasonal distribution of global marine dust dry deposition  
 (a) spring; (b) summer; (c) autumn; (d) winter



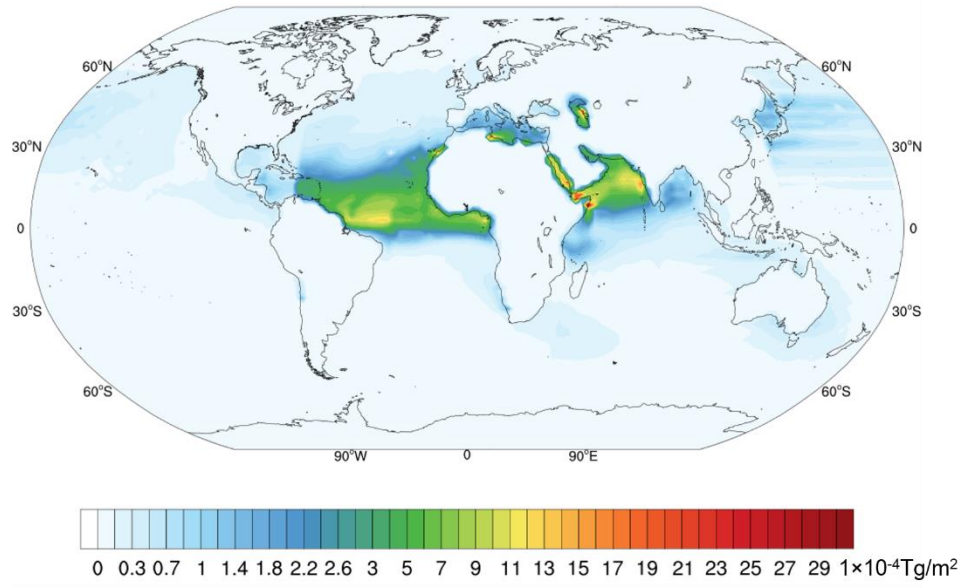
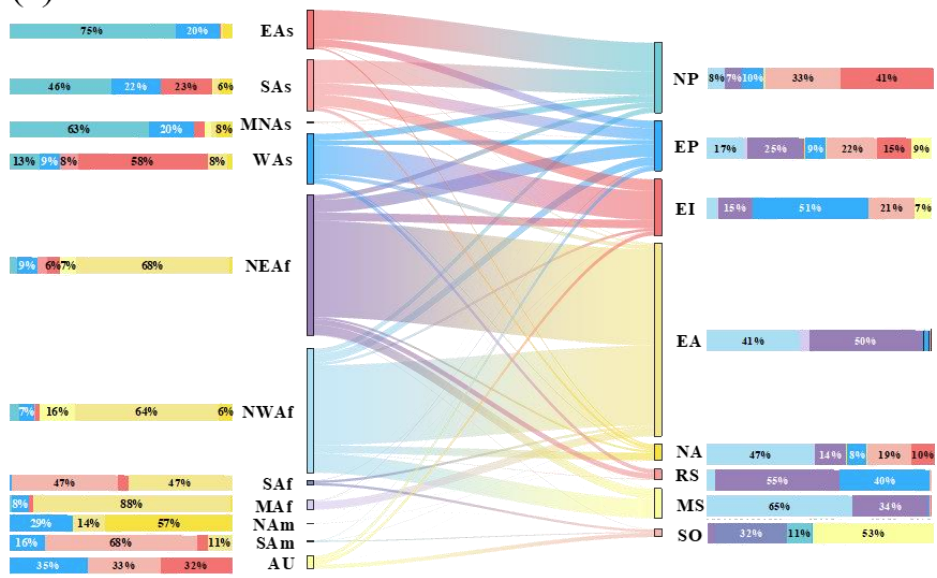
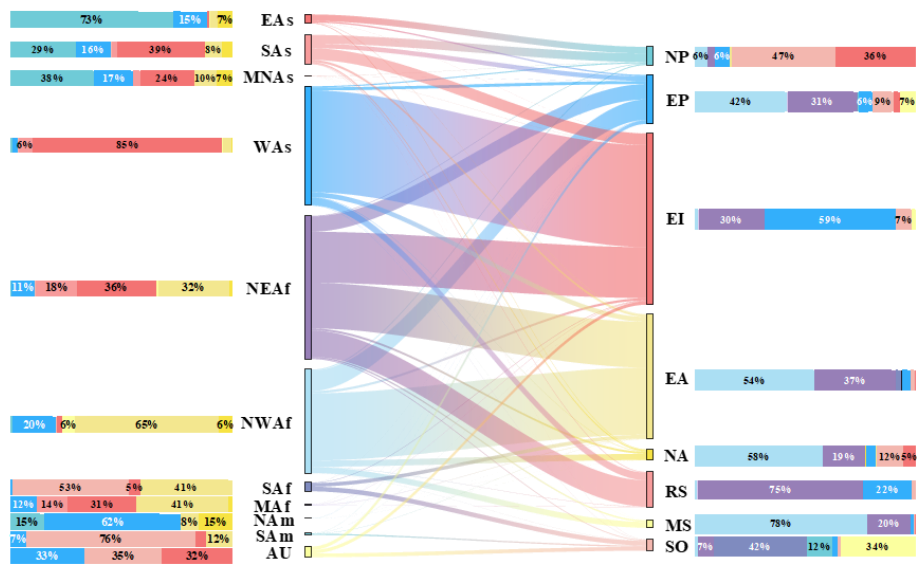


Fig. S8 The spatial distribution of dissolved iron supplied by dust deposition over global oceans

(a)



(b)



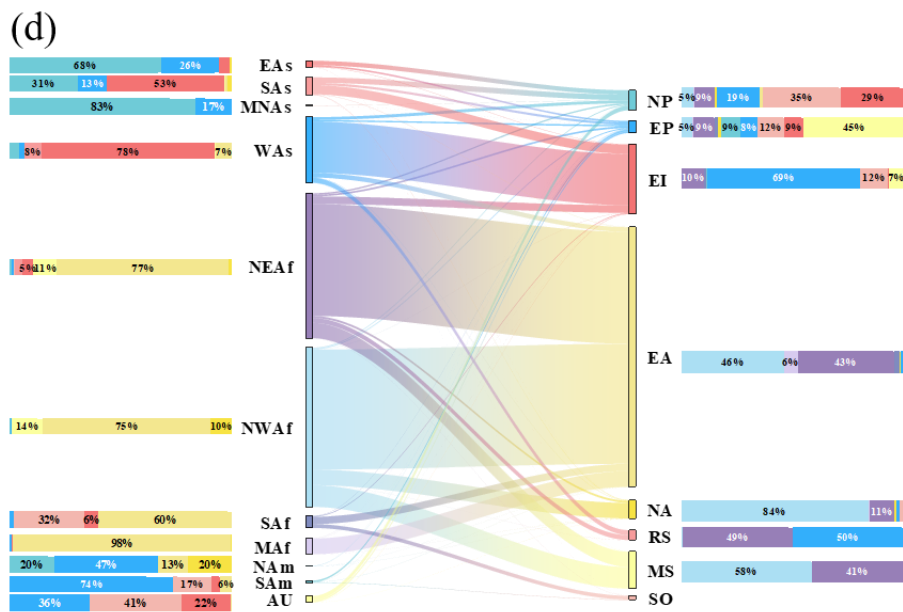
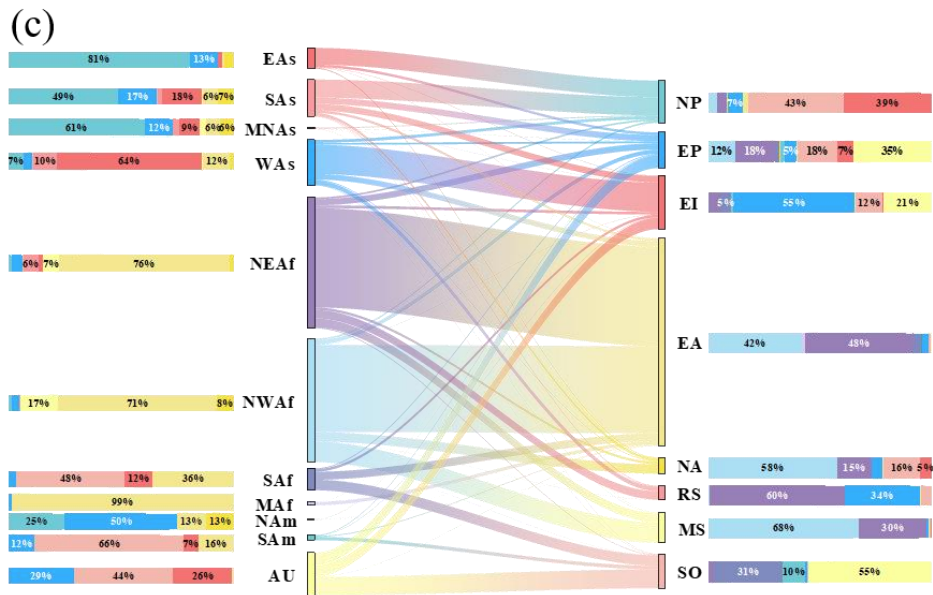


Fig. S9 The seasonal contributions of various dust source regions to oceanic dust deposition. (a) spring; (b) summer; (c) autumn; (d) winter. Each column on the left represents the fraction of dust emitted from a given source region that is ultimately deposited in individual oceans, with different colors indicating the respective oceans. Each column on the right shows the contributions of various dust source regions to dust deposition over each ocean, with different colors corresponding to different dust source regions. The longitudinal columns depict the proportions of dust emission or deposition relative to global marine dust deposition. The lines in the middle illustrate the transport direction and intensity.

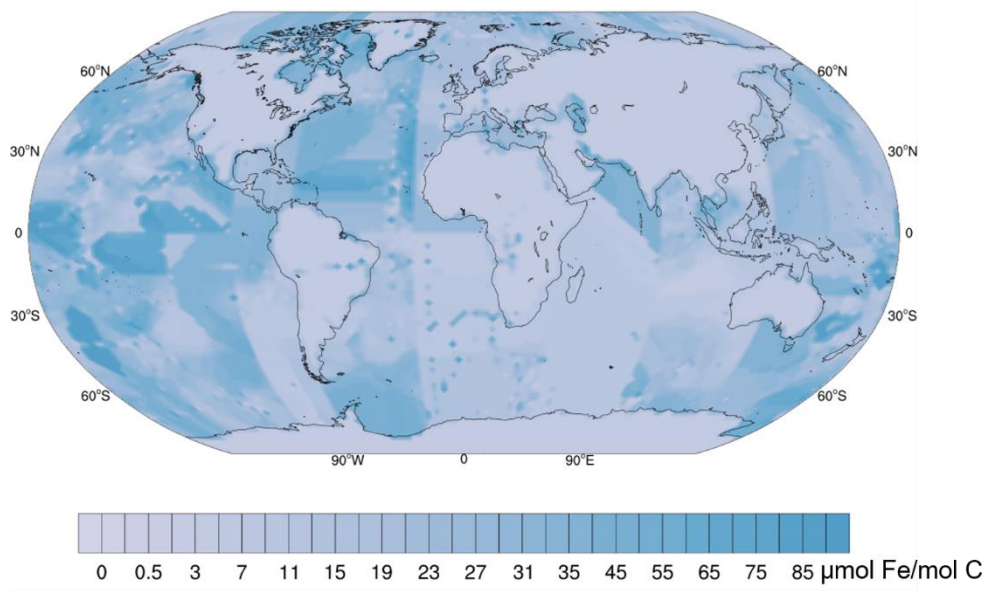


Fig. S10 The Fe: C ratio in phytoplankton cells in global oceans

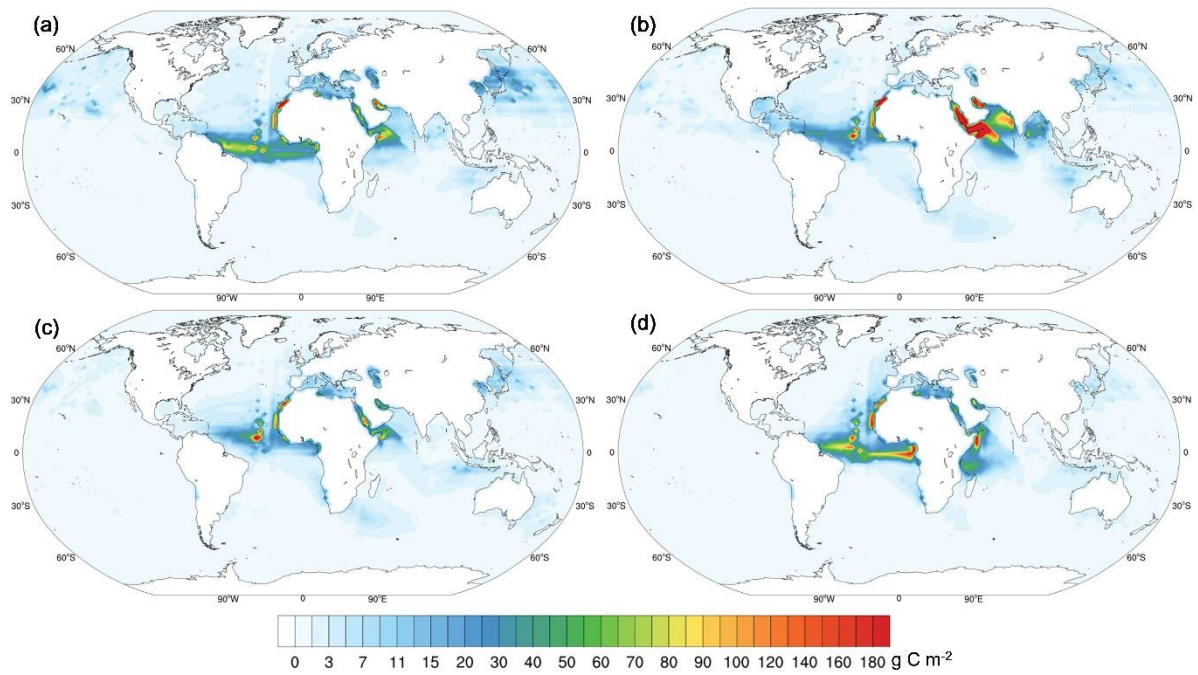
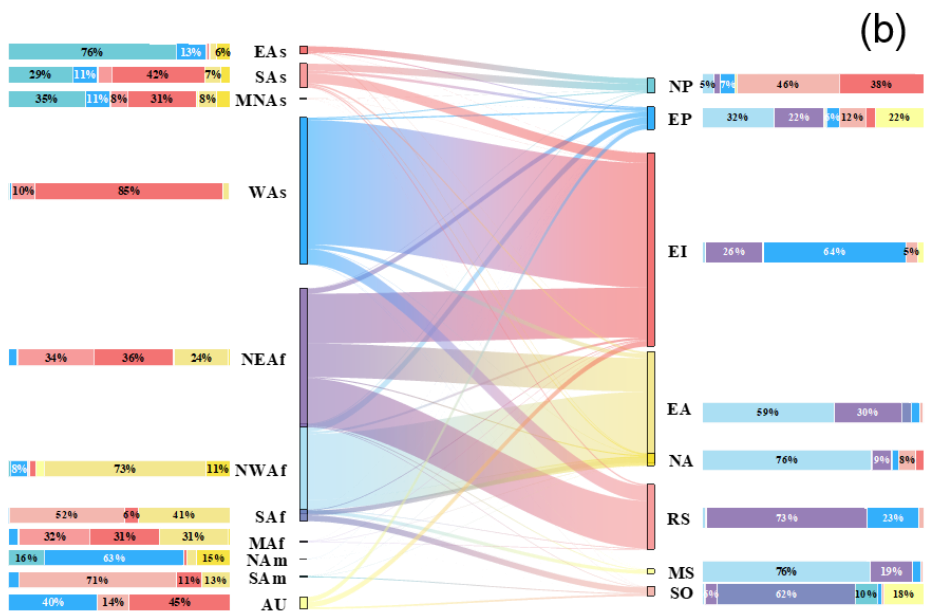
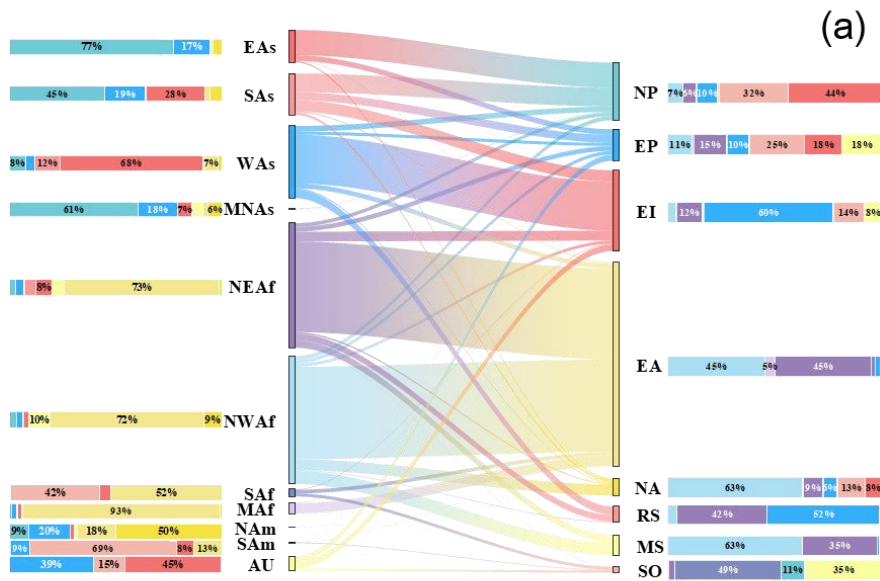


Fig. S11 The seasonal variations of marine phytoplankton carbon uptake caused by dust-borne Fe by using observed dissolved iron data, (a) spring; (b) summer; (c) autumn; (d) winter.





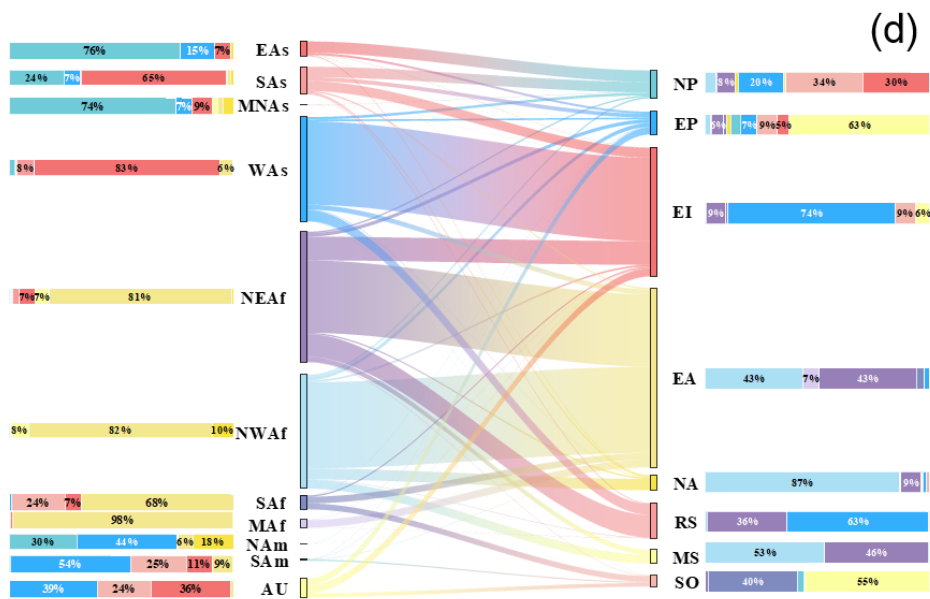
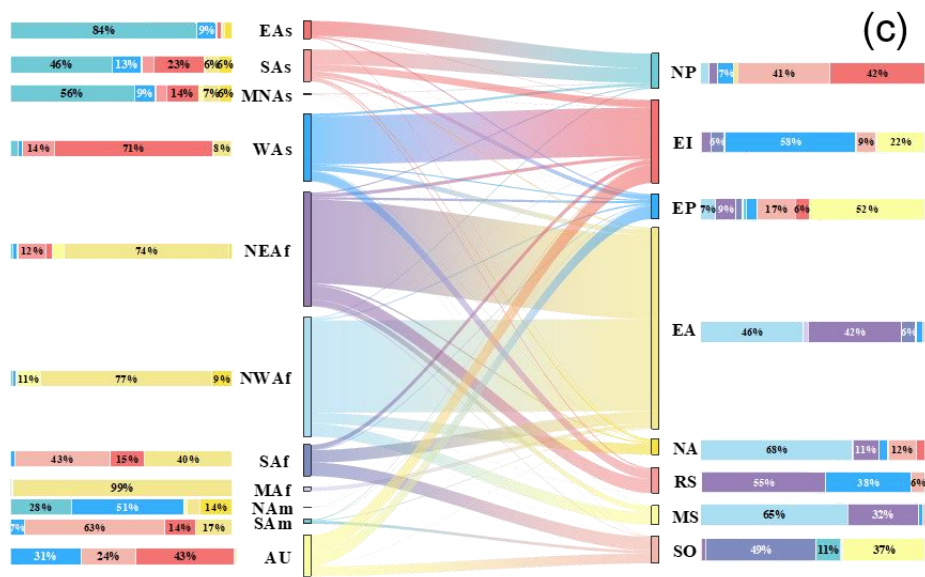


Fig. S12 The seasonal contribution of various dust source regions to the phytoplankton carbon uptake of oceans

(a) spring; (b) summer; (c) autumn; (d) winter

The left lateral columns are the proportions of dust from each dust source to induce marine phytoplankton carbon uptake over each ocean, with different colors representing different oceans. The right lateral columns illustrate the contributions from various dust sources to marine phytoplankton carbon uptake over each ocean, different color corresponding to different dust sources. The longitudinal columns display the contribution ratios of dust sources or oceans to the total marine phytoplankton carbon uptake driven by dust deposition. The lines in the middle illustrate the transport direction and intensity.



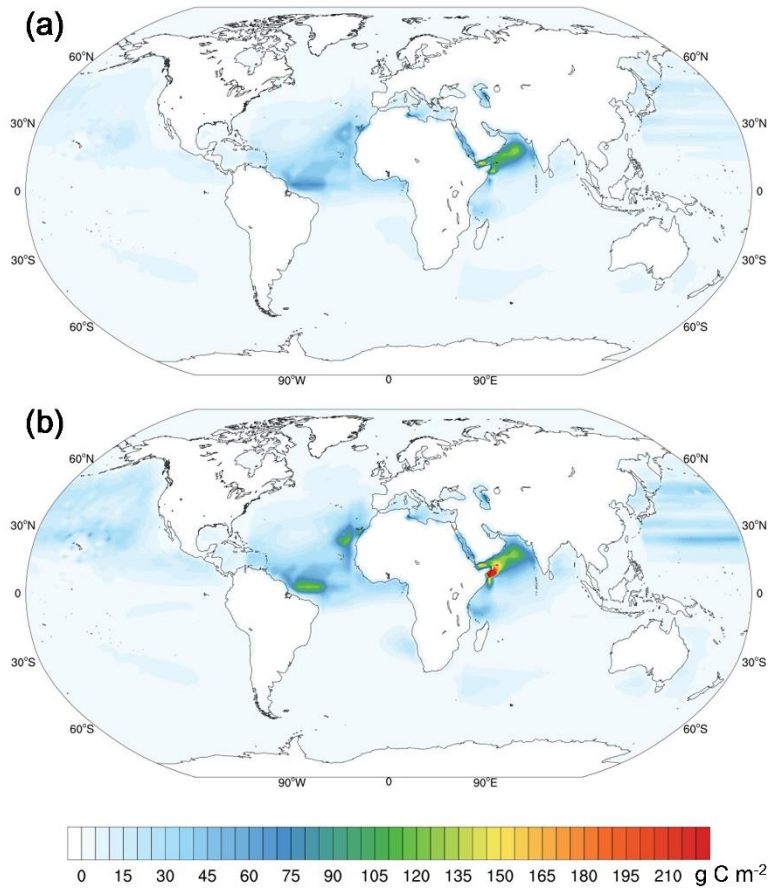


Fig. S13 The annual marine phytoplankton carbon uptake induced by dust deposition calculated by (a) CESM2 (b) GFDL-ESM4 dissolved iron data.

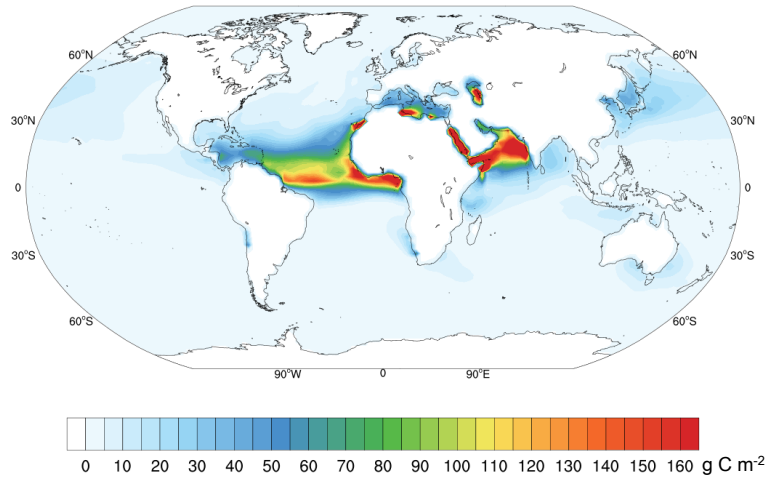


Fig. S14 Spatial distribution of annual marine phytoplankton carbon uptake driven by dust-borne iron, estimated using constant values for Fe content, iron solubility, and the Fe: C ratio in phytoplankton cells.

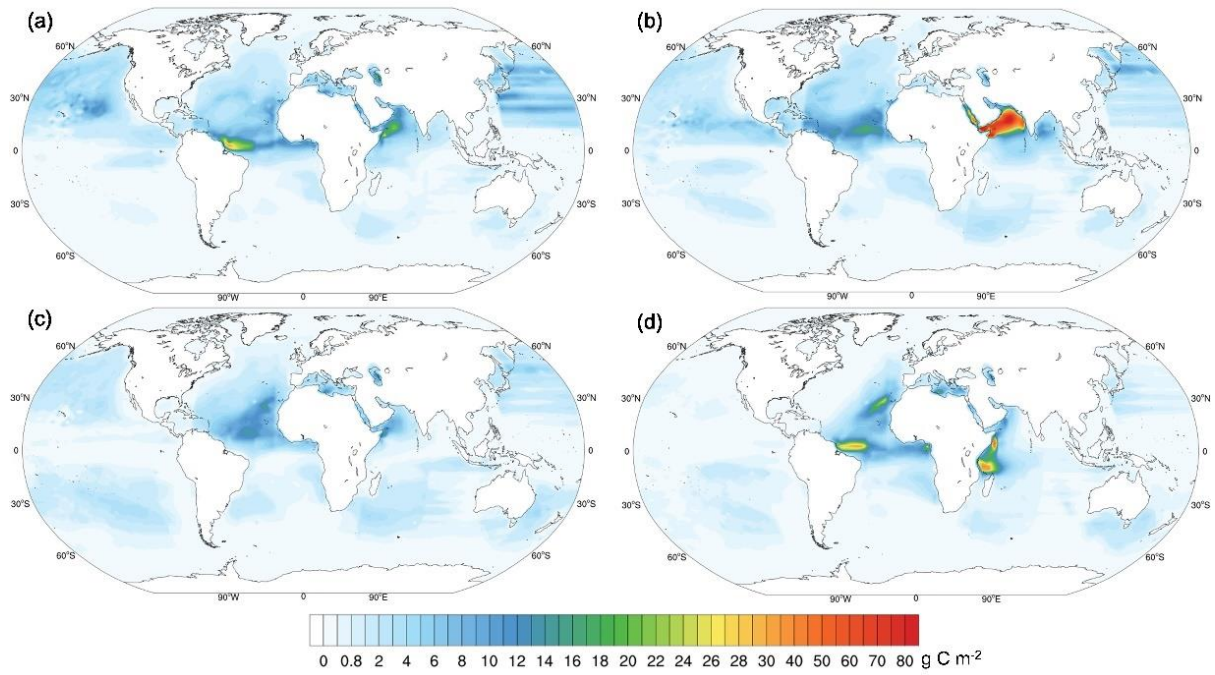


Fig. S15 Seasonal distribution of marine phytoplankton carbon uptake driven by dust-borne iron by using CESM2 dissolved iron data  
 (a) spring; (b) summer; (c) autumn; (d) winter

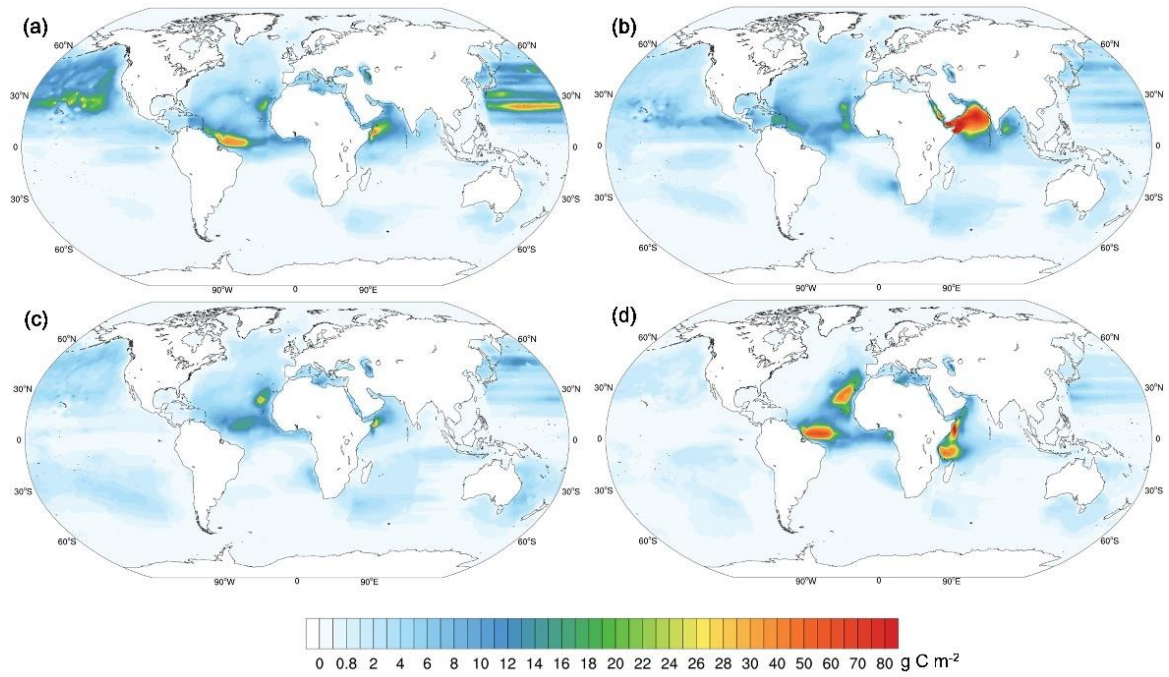


Fig. S16 Seasonal distribution of marine phytoplankton carbon uptake driven by dust-borne iron by using GFDL-ESM4 dissolved iron data  
 (a) spring; (b) summer; (c) autumn; (d) winter